

# Infrared and Raman spectroscopy of cyclohexa(*p*-phenylene sulfide) and the polymer obtained therefrom

Dean A. Zimmerman<sup>1</sup>, Jack L. Koenig, Hatsuo Ishida\*

*Department of Macromolecular Science, Case Western Reserve University, Cleveland, OH 44106-7202, USA*

Received 20 January 1998; received in revised form 24 August 1998; accepted 26 August 1998

## Abstract

The cyclic hexamer of phenylene sulfide (CHPS) is studied as a precursor of poly(*p*-phenylene sulfide) (PPS). The CHPS is one of the soluble components obtained by the extraction of poly(*p*-phenylene sulfide) with tetrahydrofuran (THF). Differential thermal analysis (DTA) is used to verify the purified cyclic compound. Fourier transform-infrared spectroscopy (FT-IR) and Raman spectroscopy are also employed. The spectra of the CHPS are compared with those of PPS and interpreted based on the symmetry of the molecules. Specifically, the C–H out-of-plane bending modes (840–800 cm<sup>-1</sup>) are indicative of the crystal structure and are utilized to identify two crystalline forms,  $\alpha$  and  $\beta$ , of the CHPS. The spectrum of the polymer obtained from the CHPS is also reported. © 1999 Elsevier Science Ltd. All rights reserved.

*Keywords:* Infrared spectroscopy; Raman spectroscopy; Poly(phenylene sulfide)

## 1. Introduction

The study of cyclic phenylene sulfides (CPSs) (Fig. 1) is important because of their potential use as polymer precursors [1,2]. Recently, there has been considerable interest in cyclic oligomers with aromatic-containing backbones for high-performance thermoplastics [3–5]. One potential benefit is that cyclic precursors would yield a polymer of high purity. Also, cyclic oligomers could lead to new reactive processing methods, since cyclics are expected to have a much lower viscosity than the polymer [5]. This is especially important for composite processing where low viscosity is needed for good fiber impregnation. Poly(*p*-phenylene sulfide) (PPS) suffers from impurities [2] and high melt viscosity, so cyclic precursors could be especially important for PPS. Spectroscopy is an important tool for studying polymerization; therefore, it is important to understand the spectra of CPSs in relationship to the polymer.

A cyclic compound provides an excellent model compound for a polymer. The only chemical difference between a CPS and the polymer is in the end-groups of the polymer, which for a molecular weight of

20 000 g mol<sup>-1</sup> results in a spectral contribution of 1%. Therefore, any appreciable differences observed in the spectra of the cyclic compound must be related to conformational or crystal structure differences. Fourier transform-infrared spectroscopy (FT-IR) and Raman spectroscopy have been used to analyze PPS [6–12], including model compound studies [7,8]. Typical model compounds are useful in assigning vibrational modes and for determining bands that are sensitive to chain length [8]; however they are not as useful in studying the effect of conformational differences. Also, in some model compound studies, there is an added influence from end-groups such as chlorine or bromine, which results in a more complicated interpretation. Therefore, the purity of the cyclic model compound is beneficial in studying the effect of conformation on the vibrational modes of the polymer.

CPSs have been detected in thermal degradation products by mass spectroscopy [13,14]. The first CPSs isolated were the tetramer ( $n = 4$ ) and pentamer ( $n = 5$ ) by Kaplan and Reents [15] from commercial PPS. The selective extraction of PPS using methylene chloride and subsequent purification has been carried out to isolate CPSs from  $n = 4$  to  $n = 8$  [16–18]. Directed synthesis of these molecules ( $n = 4, 6, 8$ ) from bithiophenylene derivatives has been performed [17], with a maximum yield of the hexamer of 73%. The cyclic hexamer of phenylene sulfide (CHPS) is the most prevalent of the CPSs and is the subject of this study.

\* Corresponding author. Tel.: +1-216-368-4172; fax: +1-216-368-4202.

<sup>1</sup> Present address: Equistar Chemicals, Cincinnati, OH 45249, USA.

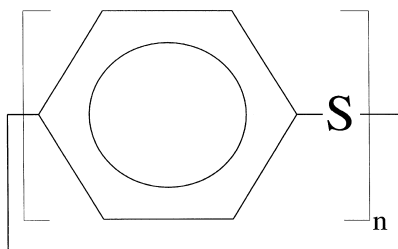


Fig. 1. Chemical structure of cyclic phenylene sulfides.

## 2. Experimental

### 2.1. Sample preparation

PPS of low molecular weight ( $M_n = 10\,000\text{ g mol}^{-1}$ ; L-PPS; Ryton V-1, Phillips) was used. PPS is insoluble in methylene chloride and tetrahydrofuran (THF), which were used to isolate the CHPS. Solvent extractions of the polymer powder were performed with methylene chloride for 12 h. The CHPS was then recrystallized from chloroform, yielding colorless needles (m.p.,  $346^\circ\text{C}$ ; literature value,  $347^\circ\text{C}$  [16]). Also, solid L-PPS was extracted with THF for 12 h. The extract was allowed to stand for five days, yielding colorless needles of the CHPS (m.p.,  $348^\circ\text{C}$ ) which were filtered and washed with solvent. In each case, the extract was filtered to remove any fine polymer powder although none was detected. KBr pellets and Nujol mulls were prepared for the FT-IR analysis.

Two types of PPS were used for the FT-IR analysis: L-PPS and the linear, higher molecular weight H-PPS (Ryton PR28, Phillips). The PPS was first extracted with THF for 18 h and dried at  $150^\circ\text{C}$  for 4 h. The washed polymer was dissolved in  $\alpha$ -chloronaphthalene (0.8 wt.%) at around  $210^\circ\text{C}$ , and several drops were placed on a thin (1 mm) KBr pellet. The pellet was heated in an argon atmosphere at  $250^\circ\text{C}$  to remove the solvent, at  $310^\circ\text{C}$  for 2 min to eliminate the thermal history, and then quenched in liquid nitrogen. The KBr was dissolved to give a thin PPS film, which was air dried and placed between KBr plates for FT-IR analysis.

### 2.2. Instrumentation

Differential thermal analysis (DTA) was performed on a Mettler FP84HT instrument. Differential scanning calorimetry (DSC) was carried out using a TA Instruments DSC 2910 according to the literature [19]. FT-IR spectroscopy was performed with use of a Bomem Michelson MB spectrometer with a liquid-nitrogen-cooled mercury–cadmium–telluride (MCT) detector at a resolution of  $2\text{ cm}^{-1}$ , unless noted. The infrared spectra in Fig. 7 were obtained with a Biorad FTS-60A spectrometer equipped with a deuterated triglycine sulfate detector. The specific detectivity,  $D^*$ , of the MCT detector was  $1 \times 10^{10}\text{ cm Hz}^{1/2}\text{ W}^{-1}$ . Raman spectroscopy was performed with a Dilor XY dispersive spectro-

meter equipped with a triple monochromator and an 18-bit, charge-coupled-device detector. The excitation source was a coherent model 890 Ti:sapphire laser at  $750.7\text{ nm}$  pumped by a coherent Innova model 305 argon ion laser. The output laser power was  $350\text{ mW}$ , the integration time was  $60\text{ s}$ , and the resolution was  $3\text{ cm}^{-1}$ .

## 3. Results and discussion

### 3.1. Isolation of the CHPS

The acetone-soluble component of the L-PPS polymer amounted to 2.5%, which is in agreement with previous work [16]. The yields of the CHPS from the extract obtained by recrystallization with chloroform and crystallization from the mother liquor were 4.8% and 0.5%, respectively. The corrected melting points from DTA measurements of the chloroform-recrystallized crystals (c-CHPS) and the THF-crystallized crystals (T-CHPS) were  $346^\circ\text{C}$  and  $348^\circ\text{C}$ , respectively. The nearest melting cyclic oligomer is the heptamer with a melting point of  $323^\circ\text{C}$  (Table 1). Also, no impurities had a melting point near that of the CHPS. Therefore, the melting point and needle shape of the crystals confirm that the hexamer ( $n = 6$ ) was obtained. Size exclusion chromatography (SEC) of the T-CHPS showed a single peak, which confirmed the purity of the CHPS. Besides the melting point, the only other difference was that the average size of the hexagonal needle crystals obtained was  $120\text{ }\mu\text{m} \times 5\text{ }\mu\text{m}$  for the c-CHPS and  $750\text{ }\mu\text{m} \times 30\text{ }\mu\text{m}$  for the T-CHPS. The higher melting point of the larger T-CHPS crystals could be due to the greater degree of crystalline perfection.

### 3.2. Spectral analysis of the CHPS

The spectra of the CHPSs are shown in Fig. 2 for crystallization from chloroform and THF. Chloroform can be observed in the c-CHPS spectrum at  $758\text{ cm}^{-1}$ . The solvent molecule is tightly bound and is still present even on heating to  $200^\circ\text{C}$  for 6 min. The entrapment of chloroform in the channels of the CHPS has been observed by X-ray measurements [20]. There is no indication of THF in the T-PPS spectrum, indicating that THF is not entrapped. The bands that are sensitive to structure in PPS [8, 12], specifically  $1573$ ,  $1180$  and  $1074\text{ cm}^{-1}$ , are enhanced in the T-CHPS compared with the c-CHPS, presumably due to the greater crystalline perfection.

To interpret the spectrum of the CHPS and compare it to the polymer, it is necessary to look at the symmetry of the molecules. The X-ray crystal structure of the hexamer has been determined by Zamaev et al. [22]. They determined that the molecule is slightly strained compared to the bond angles found in phenylene sulfide. The molecule is twisted, with the benzene rings being anywhere from planar to perpendicular to the molecular plane. The unit cell consists of stacked CHPS with channels in-between. The molecule

Table 1  
Characteristics of various cyclic *p*-phenylene sulfides [15,16]

Cyclic	$T_m$ (°C)	Crystal shape
Tetramer	296–298	Cubic
Pentamer	257–259	Needles
Hexamer	348	Needles
Heptamer	328	Cubic
Octamer	305	Needles

has a crystallographic symmetry,  $C_i$ , and the overall conformation is chair-like. Because the angles and bond lengths vary around the ring, there are no symmetry operations with respect to a given phenyl ring. If the bond lengths and angles were equal, it would possess  $C_{2v}$  symmetry. The polymer crystal has line symmetry, which is isomorphous with the  $C_{2h}$  point group. The phenyl rings of the polymer alternate  $\pm 45^\circ$  with respect to the plane containing the sulfur atoms [21]. A planar schematic of the point groups is shown in Fig. 3. Mutual exclusion holds for the crystalline polymer [8, 12], since there is a center of inversion with respect to any given phenyl ring. Band positions are given in Table 2 for the cyclic compound, and it is observed for the CHPS that the Raman and infrared bands are not mutually exclusive as expected. While there is a crystallographic center of inversion, the bands are dictated by the phenyl group, which does not have a center of inversion. The only large band shift is the symmetric ring-S stretch at  $1098\text{ cm}^{-1}$  for the cyclic compound, which occurs at  $1093\text{ cm}^{-1}$  for the polymer. The ring-S bond is known to be slightly strained in the cyclic compound compared to the polymer, which apparently results in the shift.

The spectra of quenched and annealed H-PPS are shown in Fig. 4. By comparing the spectra of CHPS and H-PPS, it can be seen that there is overall linewidth sharpening in the CHPS spectrum, which is expected for the crystalline CHPS

compared with the semi-crystalline PPS, because the semi-crystalline polymer contains amorphous material having a broader distribution of vibrational energies. Also, the bands at  $1573$ ,  $1180$ ,  $1074$ ,  $742$  and  $630\text{ cm}^{-1}$  are enhanced compared to those in the polymer spectra. These bands have been shown to decrease as the crystallinity of the polymer increases [6,8,12]. The CHPS spectrum more closely resembles the quenched PPS spectrum than the semi-crystalline spectrum. This occurs because the CHPS has a lower degree of symmetry with respect to the phenyl ring. The CHPS morphologically sensitive bands are enhanced compared with the quenched polymer because the latter can contain some localized order and some phenyl rings will have local symmetry. The CHPS molecule consists of non-symmetrically substituted phenyl rings that are fixed in position, resulting in essentially sharp, amorphous polymer-like peaks. The CHPS spectrum confirms that the bands at  $1573$ ,  $1180$ ,  $1074$ ,  $742$  and  $630\text{ cm}^{-1}$  are definitely not due to the PPS crystal lamellae but are the result of the amorphous phase.

The CHPS does not contain any impurities or branching and therefore only differs from PPS in conformation and crystal packing. The amorphous PPS most likely contains some localized symmetry. Therefore, the CHPS has less symmetry than the polymer when the phenyl group alone is considered. Because increasing symmetry should only decrease the number of fundamental bands present, the CHPS spectrum should contain all the fundamental bands of amorphous PPS except for those that can be attributed to crystal structure effects, branching or impurities. Fig. 5 shows a spectral comparison in the  $1320$ – $1140\text{ cm}^{-1}$  region scaled to the  $1472\text{ cm}^{-1}$  band. Enhancement of the  $1180\text{ cm}^{-1}$  band due to symmetry considerations is observed. Also, a very weak band at  $1232\text{ cm}^{-1}$  is observed compared with the quenched H-PPS band at  $1237\text{ cm}^{-1}$ . This band has been attributed to branching [12] in PPS and is therefore not expected in the CHPS. As a result,

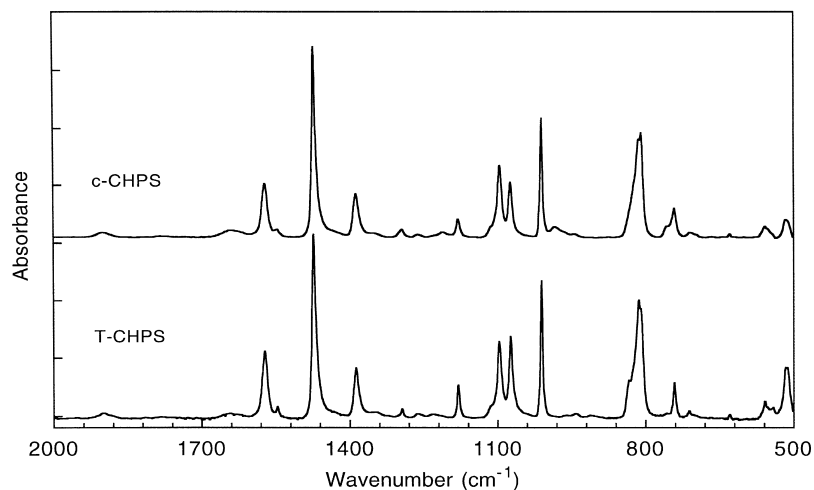


Fig. 2. FT-IR spectra of c-CHPS and T-CHPS using KBr pellets.

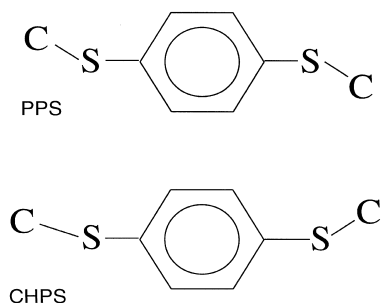


Fig. 3. Symmetry point groups of CHPS and PPS.

Table 2

Spectral comparison of CHPS with the quenched and annealed H-PPS for the region 2000–450  $\text{cm}^{-1}$  obtained at 1  $\text{cm}^{-1}$  resolution. Key: s, strong (greater than 50% intensity of maximum peak); m, medium (50–20%); w, weak (20–3%); vw, very weak (less than 3%); sh, shoulder

H-PPS quenched	H-PPS annealed	CHPS IR	PPS Raman [9]	CHPS Raman
1901, w	1907, w	1900, w		
1790, vw	1790, vw	1786, vw		
1708, vw	1708, vw			
1643, w	1640, w	1638, w		
1573, m	1573, m	1573, m	1572, m	1574, m
1549, w	1549, w	1547, w		
1472, s	1472, s	1474, s		
1440, sh	1441, sh	1438, w		
1389, m	1389, m	1388, m		
1347, w	1347, w	1348, w		
1295, w	1295, w	1294, w		
1259, w	1258, w	1263, w		
1237, w	1235, w	1232, w		
1180, w	1180, w	1180, m	1182, m	1181, m
	1118, w			
1115, w	1113, w	1115, w		
	1108, w			
1092, m	1093, s	1098, m		1097, sh
1074, m	1074, m	1074, m	1075, s	1078, s
1053, w	1054, w			
1010, s	1010, s	1011, s		
962, w	963, w	961, vw		
945, w	944, vw	942, w		
	910, w	911, w		
	825, m	835, w		
830, s	820, s	815, s		
810, b	812, sh	809, s		
742, w	742, w	742, m	742, m	742, m
	713, w	712, w		
705, w	705, sh	705, w	706, w	
651, vw				
630, vw	630, vw	631, w	629, m	630, m
567, w	567, w			
557, w	556, m	559, m	556, m	
	542, w	543, w		549, m
		518, m		
		513, m		
480, m	480, s	488, m	466, m	

there must be either a weak combination or overtone that is also present at this location. The broadness of the band in the spectrum of the crystalline material would seem to confirm this. The 1295  $\text{cm}^{-1}$  band does appear to be a fundamental band.

Furthermore, the C–H out-of-plane bending mode is significantly different. The CHPS has at least four bands compared to two in crystalline PPS (Fig. 6). The two in PPS have been assigned to the parallel and perpendicular components of the C–H out-of-plane bend [22]. Since the out-of-plane bands are sensitive to the nearest neighboring molecules, it is expected that this region shows a difference between the two materials. The band at 820  $\text{cm}^{-1}$  can be used to identify crystalline PPS.

The other significant difference is in the 600–450  $\text{cm}^{-1}$  region, which is shown in Fig. 7. This portion of the spectra shows bands that are sensitive to long-range motion. This can be noted by the fact that the cyclic compound and polymer are chemically equivalent, and yet the polymer has a band at 480  $\text{cm}^{-1}$  while the CHPS has fairly strong peaks at 543, 518, 513 and 488  $\text{cm}^{-1}$ . The bands at 518 and 513  $\text{cm}^{-1}$  may arise from crystal splitting. Other than frequency differences in the C–H out-of-plane bending mode, the band at 480  $\text{cm}^{-1}$  appears to be the most useful in distinguishing the polymer from the cyclic compound.

The Raman spectrum of the CHPS is shown in Fig. 8. Table 2 shows the frequencies obtained compared with those in the IR spectrum. As expected, there is close agreement. The sharpest feature in the Raman spectrum is the 1078  $\text{cm}^{-1}$  line. The shoulder on the higher wavenumber side is indicative of amorphous PPS [7] and is not present in the semi-crystalline PPS spectrum. This is analogous to the infrared, where the spectrum of CHPS was shown to have amorphous-like spectral features. The intensity of the structure-sensitive lines at 742 and 630  $\text{cm}^{-1}$  is much greater in the CHPS spectrum than in the PPS spectrum. Also, the lines observed in the CHPS spectrum are the same bands as those that are morphologically sensitive in the infrared. These results confirm that only modes that are sensitive to molecular conformation are present in the Raman spectrum of PPS [12].

### 3.3. Effect of heat and pressure

A change in the crystal structure has been identified in the T-CHPS and the c-CHPS crystals which is induced by heat and/or pressure. This has been confirmed by DSC, scanning electron microscopy (SEM) and optical microscopy. The crystalline form that is obtained on crystallization from solution is named the  $\alpha$ -form, while the crystalline form induced by heating or pressure is the  $\beta$ -form. The exact nature of this crystal structure change is a subject of future study; the focus here is on the spectral changes that are observed as a result of a crystal structure change.

Annealing of a KBr pellet of CHPS was carried out at

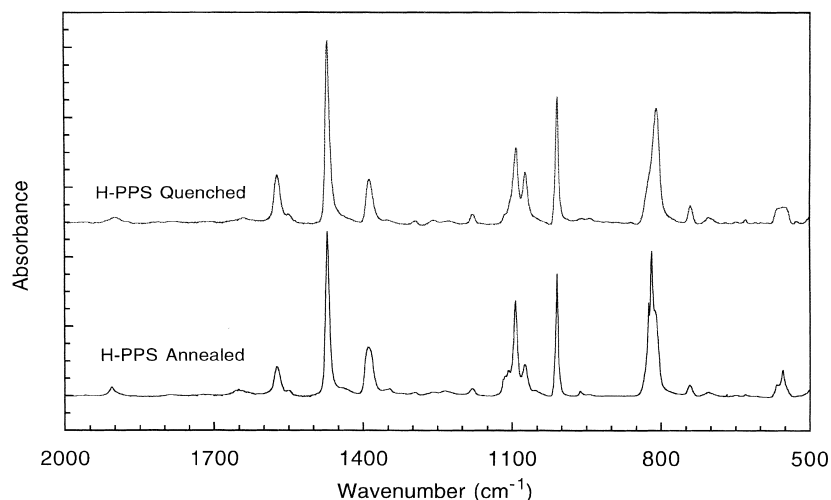


Fig. 4. FT-IR spectra of quenched and annealed H-PPS films.

250°C for 30 min. No polymerization is observed based on FT-IR spectra even after 8 h at 300°C. Therefore, the changes that are observed in the spectra are clearly due to a change in the crystal structure of the CHPS and not to opening of the ring. The spectra of the T-CHPS before and after annealing are shown along with the difference spectrum in Fig. 9. There is a significant change in the C–H out-of-plane bending region, which is sensitive to its nearest neighbors and is therefore most indicative of a crystal structure change. Fig. 10 shows this spectral region before and after annealing of the CHPS. Since the bands are highly overlapping, curve resolution was used. Table 3 summarizes the band positions obtained for the polymer and the CHPS. On the annealing of the CHPS, the emergence of bands at 833, 826 and 803  $\text{cm}^{-1}$  can be seen. The band at 803  $\text{cm}^{-1}$  is especially distinct. This band does not significantly overlap with bands from the  $\alpha$ -form or the polymer and can be used to identify the  $\beta$ -form.

Also, there is a significant reduction in intensity of the crystallinity-sensitive modes at 543, 518, 513 and 488  $\text{cm}^{-1}$ . Apparently, the long-range order is disrupted due to the crystal structure change. The number of bands in this region also increases dramatically, probably due to crystal field splitting. Splitting can also be observed for the C–H in-plane deformation modes at 1011 and 1180  $\text{cm}^{-1}$ . The band at 1011  $\text{cm}^{-1}$  shows little sensitivity to structure; therefore the significant reduction in intensity must be related to broadening of the peak or splitting, of which the latter seems to occur.

The structural change can also be pressure-induced. It was observed that 24 h after pressing a KBr pellet, an indication of the same structural change as that obtained by annealing could be seen. The spectrum of the CHPS in a KBr pellet even shows some changes immediately after pressing. This is shown in Fig. 11 for the T-CHPS using a KBr pellet compared with using a mull for two regions that

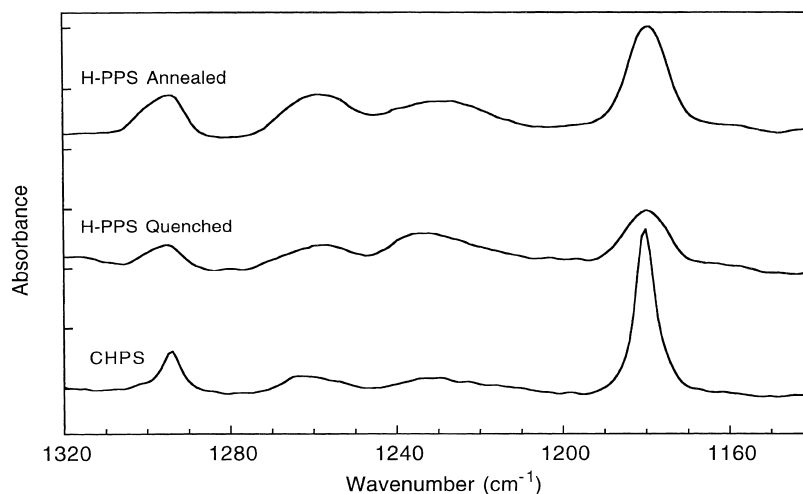


Fig. 5. FT-IR spectral comparison of quenched and annealed PPS with the cyclic compound in the 1320–1140  $\text{cm}^{-1}$  region.

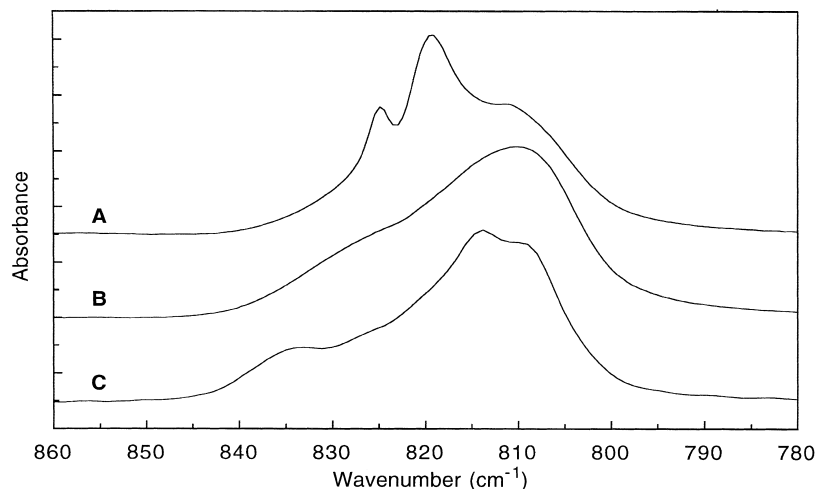


Fig. 6. Comparison of the C–H out-of-plane bending region for (A) H-PPS annealed, (B) H-PPS quenched and (C) T-CHPS.

are sensitive to crystal packing. Although they are both obtained at a resolution of  $2\text{ cm}^{-1}$ , the peaks are better resolved in the mull spectrum. There is essentially no change in the rest of the spectra other than in these two regions.

### 3.4. Polymerization of the CHPS

Polymerization of CHPS was carried out by heating a KBr pellet to  $330^\circ\text{C}$  in air and slowly cooling (about 1 h) to  $260^\circ\text{C}$ , followed by annealing for 16 h. The pellet was repressed and the spectrum obtained. Pressing appeared to have no effect on the spectrum, except to improve the spectral quality. No attempt was made to study the polymerization process; rather, a polymerized product for spectral comparison was the goal. The spectra of the polymer from cyclic oligomers (CO-PPS) and annealed L-PPS are shown in Fig. 12. From the spectra it can be clearly seen that polymer was obtained, which was confirmed by DSC

(m.p.  $280^\circ\text{C}$ ). DSC was also used to estimate the molecular weight. Fagerburg et al. [19] have reported that the logarithm of the glass transition temperature is directly proportional to the molecular weight up to a degree of polymerization of 200. The amount of undercooling (crystallization temperature during cooling,  $T_{cc}$ , subtracted from the melting temperature,  $T_m$ ) can also be used. The difference between  $T_{cc}$  and  $T_{ch}$ , the crystallization temperature during heating, indicates the relative rate of crystallization and is also an indication of the molecular weight. The molecular weight of the polymerized CHPS was estimated to be  $6000\text{ g mol}^{-1}$ . The results are summarized in Table 4.

The FT-IR spectrum of the CO-PPS reveals several characteristics. First, there is little branching as expected based on the very weak  $1232\text{ cm}^{-1}$  band [12]. The L-PPS band at  $1235\text{ cm}^{-1}$  is considerably greater in intensity than either in the CO-PPS or the H-PPS, in which it appears to be about the same. A weak band can be detected in the difference

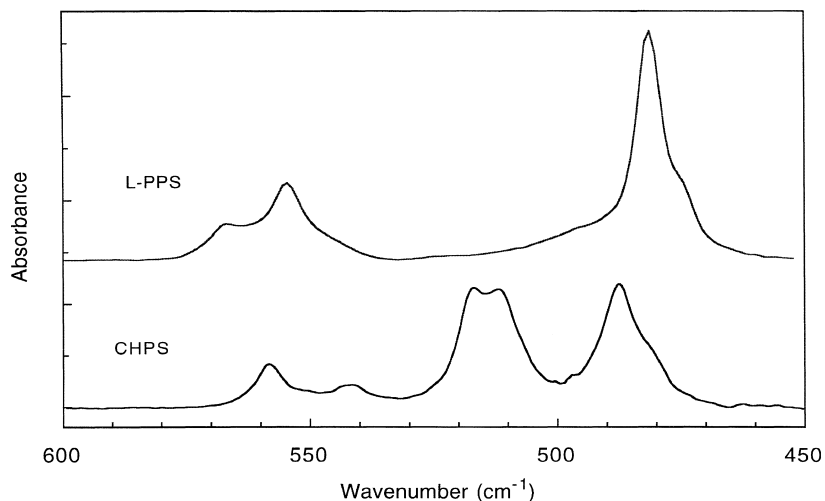


Fig. 7. FT-IR spectra of annealed L-PPS and T-CHPS from  $600$  to  $450\text{ cm}^{-1}$ .

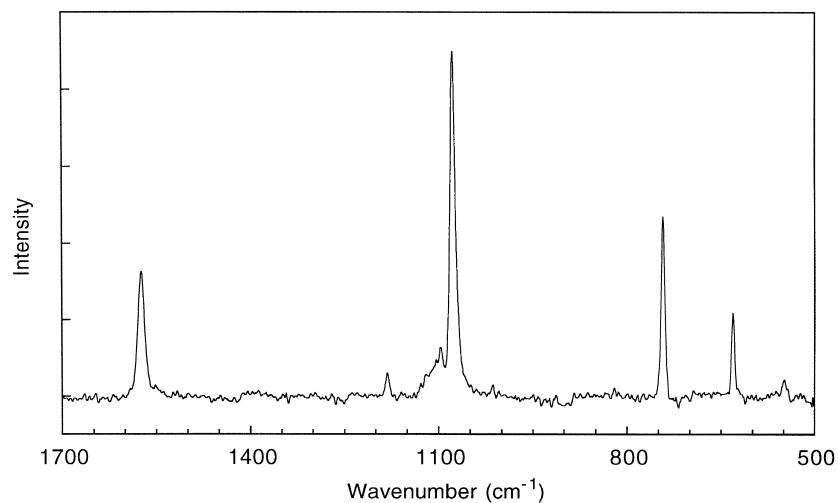


Fig. 8. Raman spectrum of T-CHPS.

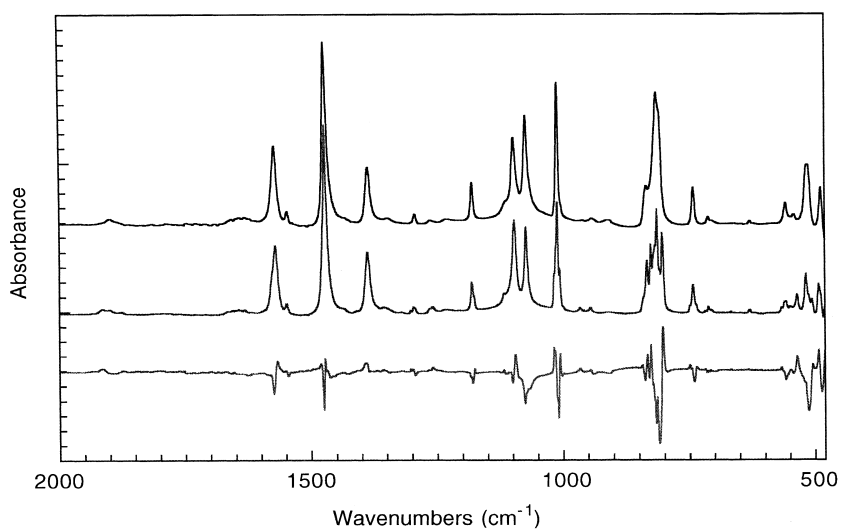


Fig. 9. Comparison of the FT-IR spectra of T-CHPS before and after annealing including the subtraction spectrum.

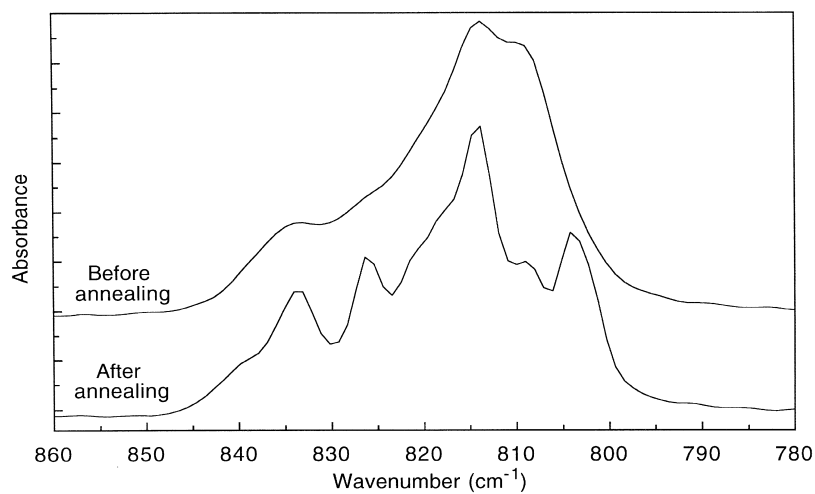


Fig. 10. Comparison of the C–H out-of-plane deformation FT-IR spectral region before and after annealing of T-CHPS.

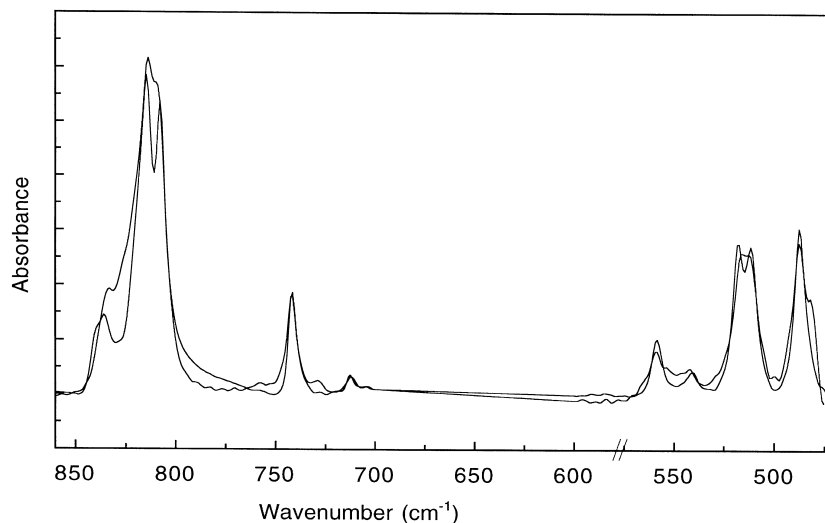


Fig. 11. Overlay of the FT-IR spectra of T-CHPS obtained with a KBr pellet and a mull at  $2\text{ cm}^{-1}$  resolution. The mull spectrum results in the sharper peaks.

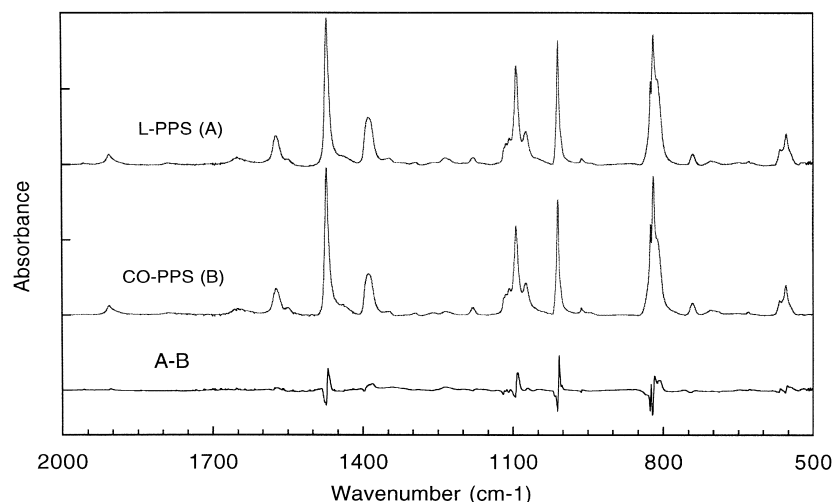


Fig. 12. FT-IR spectra of the polymerized product of CHPS (CO-PPS), annealed L-PPS, and the subtraction spectrum.

spectrum. It is expected that the reaction is highly selective, since there are reactive para end sites which should be favored over the meta or ortho sites. Also any branches that would occur would be a minimum of six units long.

Table 3

Curve resolved band positions ( $\text{cm}^{-1}$ ) in the C–H out-of-plane bending region from  $850$  to  $790\text{ cm}^{-1}$

Quenched PPS	Annealed PPS	CHPS	Annealed CHPS
810 <sup>a</sup>	811	808	803
823	820 <sup>a</sup>	814 <sup>a</sup>	809
	825	818	814 <sup>a</sup>
		835	818
		840	821
			826
			833
			842

<sup>a</sup> Most intense peak.

Furthermore, the relative degree of crystallization can be ascertained by comparing the ratio of intensities of three sets of peaks [12]: the crystalline to amorphous C–H out-of-plane bending bands at  $820$  and  $812\text{ cm}^{-1}$ , the symmetric to antisymmetric ring–S stretch bands at  $1093$  and  $1074\text{ cm}^{-1}$ , and the ring stretching modes at  $1472$  and  $1573\text{ cm}^{-1}$ . The intensities were obtained by curve

Table 4

Summary of molecular weights obtained by DSC for PPS from cyclic oligomers

Parameter	Temp. ( $^{\circ}\text{C}$ )	Molecular weight ( $\text{kg mol}^{-1}$ )
$T_g$	86	5.7
$T_m - T_{cc}$	58	5.6
$T_{cc} - T_{ch}$	79	6.7



Table 5  
Spectral comparison of low and high molecular weight PPS with PPS obtained from cyclic oligomers (CO-PPS) using curve-fitted intensities

Polymer	Ratio of peak intensities <sup>a</sup>		
	1472/1573	1093/1074	820/812
H-PPS	5.68	3.51	1.13
CO-PPS	5.40	3.20	1.07
L-PPS	4.15	2.80	0.96

<sup>a</sup>A higher ratio is indicative of higher crystallinity.

resolving the bands. The results are summarized in Table 5. Presumably, the higher degree of branching in the L-PPS limits the amount of crystallization that can occur. Therefore, the CO-PPS has a greater degree of crystallization, although it has a lower molecular weight. The H-PPS has the highest degree of crystallization, which is expected based on molecular weight effects. The ratio of the intensity of the band at 1074 to 1093  $\text{cm}^{-1}$  has been correlated with DSC data to estimate the per cent crystallinity [23], which is 62%, 59% and 56% for the H-PPS, CO-PPS and L-PPS respectively. The values are estimates because they are not correlated with X-ray diffraction values.

#### 4. Conclusions

The spectra of CHPS have been related to the spectra of PPS and closely resemble that of amorphous PPS, due to its lower degree of symmetry compared to the polymer crystal. Specific modes indicative of the crystal structure and band shifts have been reported. A crystal structure change in the CHPS has been identified which is induced by pressure or heat. Polymerization of the CHPS has been performed and the corresponding changes in the spectra have been identified. The polymerized CHPS is found to have slightly higher crystallinity compared to the commercial, low-molecular-weight PPS with minimal branching.

#### Acknowledgements

The PPS was graciously supplied by the Phillips Petroleum Company. This work was sponsored in part by a grant from the Office of Naval Research.

#### References

- [1] Nedel'kin VI, Zhorin VA, Astankov AV, Sergeev VA, Enikolopov NS. *Polym Sci, Ser B* 1993;35:1282.
- [2] Nedel'kin VI, Astankov AV, Sergeev VA. *Dokl Phys Chem* 1993;326:496.
- [3] Ganguly S, Gibson HW. *Macromolecules* 1993;26:2408.
- [4] Brunelle DJ, Shannon TG. *Macromolecules* 1991;24:3035.
- [5] Mullins MJ, Woo EP, Murray DJ, Bishop MT. *Chemtech* 1993;23:25.
- [6] Piaggio P, Cuniberti C, Dellepiane G, Capannelli G. *Synth Methods* 1989;29:E61.
- [7] Pan Z, Savard T, Wicksted JP. *J Raman Spectrosc* 1992;23:615.
- [8] Piaggio P, Cuniberti C, Dellepiane G, Campani E, Gorini G, Masetti G, Novi M, Petrillo G. *Spectrochim Acta, Part A* 1989;45:347.
- [9] Radhakrishnan S, Nadkarni VM. *Polym Eng Sci* 1984;24:1383.
- [10] Zhang G, Wang Q, Yu X, Su D, Li Z, Zhang G. *Spectrochim Acta, Part A* 1991;47:737.
- [11] Zeraoui S, Buisson JP, Mevellec JY, Lefrant S. *Synth Methods* 1993;55:487.
- [12] Zimmerman DA, Ishida H. *Spectrochim Acta, Part A* 1995;51:2397.
- [13] Montaudo G, Puglisi C, Scamporrino E, Vitalini D. *Macromolecules* 1986;19:2157.
- [14] Reents WD, Kaplan ML. *Polymer* 1982;23:310.
- [15] Kaplan ML, Reents WD. *Tetrahedron Lett* 1982;23:373.
- [16] Sergeev VA, Nedel'kin VI, Astankov AV, Yunnikov VV, Erzh BV. *Dokl Phys Chem* 1989;304:114.
- [17] Sergeev VA, Nedel'kin VI, Astankov AV, Nikiforov AV, Alov EM, Moskvichev YuA. *Bull Acad Sci USSR* 1990;39(4):763.
- [18] Sergeev VA, Nedel'kin VI, Astankov AV. *Bull Acad Sci USSR* 1987;36(8):1770.
- [19] Fagerburg DR, Watkins JJ, Lawrence PB. *Macromolecules* 1993;26:114.
- [20] Zamaev IA, Shklover VE, Struchkov YuT, Astankov AV, Nedel'kin VI, Sergeev VA, Ovchinnikov YuA. *J Struct Chem* 1990;31:519.
- [21] Tabor BJ, Magré EP, Boon J. *Eur Polym J* 1971;7:1127.
- [22] Neyman G. PhD Thesis. Case Western Reserve University, 1994.
- [23] Cole KC, Noël D, Hechler J-J. *J Appl Polym Sci* 1990;39:1887.